Experimental Study of Composite Cold-Formed Steel Trusses in Floor Systems Subjected to Cyclic Loading

*Ashraf ElSabbagh [1], Mohamed Hammam [2, *], Mohamed Elghandour [3], Tarek Sharaf [4]*

[1] *Associate Prof, Civil Engineering Department, Faculty of Engineering, Port Said University, Port Said, Egypt,*

E-mail: ashref.ismail@eng.psu.edu.eg

[2] *Master Student, Civil Engineering Department, Faculty of Engineering, Port Said University, Port Said, Egypt,*

E-mail: mohamed.alaraby@eng.psu.edu.eg

[3] *Professor, Civil Engineering Department, Faculty of Engineering, Port Said University, Port Said, Egypt,*

E-mail: dr.elghandor@gmail.com

[4] *Associate Prof, Civil Engineering Department, Faculty of Engineering, Port Said University, Port Said, Egypt,*

E-mail: tarek.sharaf@eng.psu.edu.eg

Corresponding author, DOI: 10.21608/PSERJ.2024.333409.1377

ABSTRACT

Composite Cold-Formed Steel (CFS) trusses are increasingly used in building construction due to their high strength-to-weight ratio, making them ideal for long spans. However, their behavior under cyclic loads remains an important research area. Therefore, this study investigates the behavior of CFS trusses under cyclic loading. The primary aim is to study the factors affecting the behavior of composite CFS trusses, such as the thickness of truss members, type of shear connector, thickness of gusset plates, and type of truss. Sixteen full-scale composite CFS truss models were tested and investigated in terms of load-carrying capacity, failure mechanism, maximum deformation, and interaction between the concrete slabs and CFS trusses. Additionally, this study proposes four new solutions for bolted CFS shear connectors. Nine push-out specimens were tested to investigate the behavior of the proposed connectors in terms of shear capacity, maximum displacement, and failure mechanism. The results of the full-scale models showed that the behavior of the composite CFS trusses was mainly affected by the thickness of the gusset plates. The results of the push-out specimens were used to develop design equations that could be used to calculate the shear capacity of the proposed connectors.

Keywords: Composite floor systems, Cold-formed steel trusses, Cyclic loading, Shear connectors, Experimental study, Full-scale tests.

NOMENCLATURE

A_{eff}	Effective area of the CFS section to resist buckling due to compression
A_g	Gross area of the CFS section
A_{net}	Net area of the CFS section to resist rupture due to tension
A_{tr}	Total area of the transversal rebars in the TWP
b_e	Effective width of the slab
d	Diameter of the TWP holes
d_v	Vertical displacement of the full-scale composite truss models
d_{vmax}	Maximum vertical deformation of the full-scale models
d_{vs}	Vertical displacement of push-out tests
d_{vsmax}	Maximum vertical displacement of push-out tests
E_{cm}	Secant modulus of elasticity of concrete
E_s	Modulus of elasticity of steel
ε_y	Yield strain of steel
f_{ck}	Cylinder compressive strength of concrete
f_y	Yield stress of steel
f_u	Tensile strength of steel
h_c	Height of the TWP
L, L_1, L_2	Lengths of full-scale models
L_c	Length of the connector
η	Degree of interaction
n_c	Number of shear connectors at the maximum shear zone
n_f	Number of shear connectors required for full interaction
n_h	Number of the holes in the TWP

P_{act}	Actuator load at the failure
P_d	Calculated design load
P_{sw}	Self-weight load of both the full-scale model and transversal beams
P_u	Total experimental load (actuator and self-weight loads)
Q_d	Design capacity of the connector
Q_u	Experimental capacity of the connector
R_c	Maximum compressive force acting on the concrete
R_q	Total capacity of shear connectors at the maximum shear zone
R_t	Maximum tensile force acting on the bottom chord
t_c	Thickness of the TWP
t_f	Flange thickness of the channel
t_s	Thickness of the slab
t_w	Web thickness of the channel

1 INTRODUCTION

Concrete floor systems have been the most enduring and widely used structural systems over time. However, hot-rolled steel sections are suitable for application in concrete floor systems. This system is commonly referred to as the composite floor system [1]. Significant interaction between steel and concrete is required to enhance the structural behavior of composite steel systems. The referred-to interaction can be achieved by using shear connectors. The most common type of shear connector is steel stud shear connectors that are welded to the top flange of the steel beam [2]. Many researchers have investigated the behavior of composite steel joist floor systems with shear connectors. Wang et al. [3] conducted four experimental tests to study the performance of both composite and bare steel joists. The findings proved that composite joists showed higher capacity and lower deformation compared to bare steel joists. Azmi et al. [4] experimentally studied the behavior of composite open-web joists with welded shear studs. The results declared that welded shear studs could be used as shear connectors as they provided full interaction. Fahmy et al. [5] conducted analytical models to analyze the behavior of composite steel joists with shear studs and the puddle-welds. Sharaf et al. [6] experimentally studied the behavior of composite T-beams. Muhammad [7] and Merryfield et al. [8] experimentally investigated the ability to use puddle-

welds and Hilti-screws as shear connectors in composite steel joists. The findings indicated that puddle-welds could be used as shear connectors. However, Hilti-screws couldn't be used as they didn't provide significant interaction. Abduljabbar et al. [9] experimentally investigated the behavior of composite open-web steel joists with ordinary welded shear studs under monotonic loading. The results indicated that reducing the span-to-depth ratio increased the capacity of the composite joists. Another type of composite floor system that is recently used is cold-formed steel (CFS) instead of hot-rolled sections. The utilization of CFS composite floor systems has become common in many permanent structures, including residential and multi-story buildings. The referred-to floor system consists of wood-based panels connected to CFS beams with self-drilling screws [10]. The main problem associated with this floor system is the lack of shear connectors to provide significant interaction between the steel and concrete. The use of welded shear studs in this floor system can reduce the thickness of the top flange. As the beam thickness decreases, the utilization of welded shear studs becomes increasingly challenging due to the risk of harmful impacts on the top flange, such as damage or burning [11]. To find suitable solutions for shear connectors in the composite CFS floor system, many researchers conducted studies and experiments on different types of shear connectors that didn't require welding procedures. Dabaon et al. [12]–[15] conducted experimental and analytical studies on three types of CFS shear connectors. Wehbe et al. [16] experimentally studied the possibility of using stand-off screws as shear connectors. Based on the results, proper spacing and number of screws should be used to achieve the desired composite action. Hsu et al. [17] proposed and tested a new composite system with a continuous cold-formed furring shear connector with a bent rib on the lips. The findings indicated that the proposed system could be used as a shear connector. Bamaga et al. [18] conducted experimental push-out tests on CFS specimens with three different types of shear connectors bolted to the web of the beam. The findings showed that the proposed

connectors had higher shear capacity and ductility than the ordinary welded shear studs. Leal et al. [19] proposed and tested three types of CFS connectors connected to the trussed beam top chord with self-drilling screws. The results showed that the proposed connectors could provide full interaction. Hosseinpour et al. [20] conducted an experimental investigation on the behavior of bolted shear connectors in composite cold-formed steel beams as a suitable alternative to welded shear studs. Previous research showed that CFS joists and trussed beams can be used in structural systems. However, it is worth noting that the real truss system can support higher loads over longer spans due to its high strength-to-weight ratio [21]. The main limitation that hinders the utilization of the CFS truss system is the weakness of connections between its members. The insignificant thickness of the CFS gusset plates can result in premature failure at the truss joints before reaching the maximum load-carrying capacity of the composite floor system [22]. Few researchers studied the effect of gusset plates on the behavior of composite CFS trusses. Reda et al. [23] analytically studied the behavior of CFS roof trusses. Padmanaban et al. [24] conducted experimental tests on three small-scale CFS trusses. The findings indicated that the stiffness of the gusset plates had a significant effect on the capacity of CFS trusses. Ammar et al. [25] experimentally studied the effect of gusset plate thickness on the behavior of CFS trusses. The results declared that increasing the thickness of gusset plates increased the capacity of the truss and changed the failure mechanism from premature failure of joints to buckling failure of members. Based on the findings of previous research, the main aim of this study is to investigate the effect of the gusset plate thickness, member thickness, and truss type on the behavior of CFS composite trusses. Sixteen full-scale composite CFS truss models were tested and investigated in terms of load-carrying capacity, failure mechanism, maximum deformation, and interaction between the concrete slabs and CFS trusses. Additionally, this study proposes four new solutions for CFS shear connectors in composite floor systems. Nine push-out specimens were tested to investigate the behavior of the proposed connectors in terms of shear capacity, maximum displacement, and failure mechanism.

2   MATERIAL PROPERTIES

Table 1 shows the mechanical properties of CFS and the concrete used in both full-scale models and push-out specimens. CFS grade and plate thickness were chosen according to the available materials at the local market. The mechanical properties of CFS were determined based on the tensile coupon tests, while the mechanical properties of concrete were determined based on the results of compressive tests on standard cubes. The used M8 bolts had a grade of 8.8 with a yield stress of 640 MPa and a tensile strength of 800 MPa. Furthermore, both the reinforcement steel mesh and TWP transversal rebars had a yield stress of 240 MPa and ultimate tensile strength of 360 MPa.

3   SHEAR CONNECTORS

Shear connectors are used to prevent the separation of the slab during the tests by providing significant interaction between CFS and concrete. Figure 1(a) shows a top chord with an inverted lipped channel. In this case, the lips of the channel can act as a shear connector after the slab is cast, and the top chord is filled with concrete. Figure 1(b) shows a thin-walled perfobond (TWP) shear connector consisting of two CFS angles (L90×30 mm) connected with M8 bolts, along with three φ8×600 mm transversal reinforcing steel rebars. Figure 1(c) shows a thin-walled channel (TWC) shear connector consisting of a CFS lipped channel (C80×60×20).

Table 1. Mechanical properties of CFS and the concrete used in models and specimens

Steel				Concrete	
Modulus of Elasticity E_s (MPa)	Yield Stress f_y (MPa)	Tensile Strength f_u (MPa)	Yield Strain E_y (μstr)	Compressive Strength f_{ck} (MPa)	Secant Modulus of Elasticity E_{cm} (MPa)
185,800	340	440	1830	20	29,962
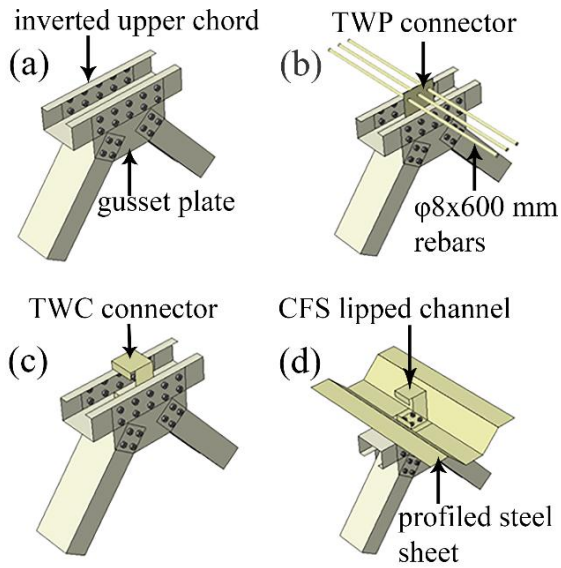
Figure 1: Proposed CFS shear connectors; a) inverted top chord, b) TWP, c) TWC, and d) ordinary top chord with profiled steel sheet and CFS lipped channel

Figure 1(d) shows an ordinary top chord with a profiled steel sheet and CFS lipped channels (C80×60×20) used as shear connectors. All shear connectors have a uniform thickness of 1.5 mm and are connected to the top chord with M8 bolts instead of using welding procedures. The use of bolts instead of self-drilling screws is to prevent the possibility of pull-out failure during the experimental tests. The validity of the proposed connectors was studied by the full-scale tests, while their shear capacity was determined by the push-out tests.

4 PUSH-OUT TESTS

4.1 Specimens: Fabrication and General Details

The main objective of the push-out tests is to study the behavior of the proposed shear connectors in terms of shear capacity, maximum displacement, and failure mechanism. To achieve this objective, nine push-out specimens were manufactured and tested according to the recommendations of Eurocode 4 [26]. So that, the push-out specimens were adjusted to simulate the concrete slab slippage of full-scale models. Three push-out specimens were manufactured for each type of shear connector (types B, C, and D). Based on the test results of the full-scale models, the proposed type A shear connectors (with an inverted top chord only) didn't

provide significant interaction between CFS and concrete, as the concrete slab cracked and partially separated from the CFS truss before the truss reached its maximum load-carrying capacity. Therefore, no push-out specimens were manufactured for the proposed type A shear connectors. The dimensions as well as the details of the TWP (Type B) push-out specimen are shown in Figure 2 and Figure 3, respectively. The referred-to specimen is composed of two concrete solid slabs and a load distribution member manufactured with two CFS lipped channels (C100×60×20×3.0 mm). The thickness of the referred-to member was taken at 3.0 mm to prevent buckling failure of the CFS member during the push-out tests. The load distribution member is only inverted in specimens with TWP and TWC connectors. However, for all specimens, the slabs have the same thickness and reinforcement as the full-scale models.
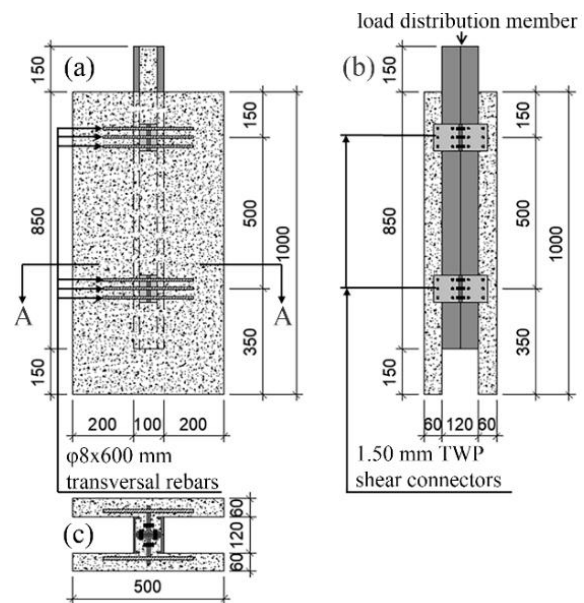
Figure 2: TWP (Type B) push-out specimen (dimensions in mm); a) section elevation, b) section side view, and c) section plan at A-A
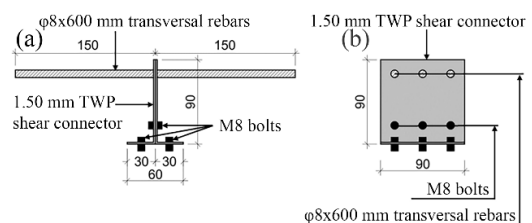
Figure 3: Details of the TWP (Type B) connectors; a) elevation, and b) side view

4

The concrete slabs dimensions were 1000×500×60 mm, respectively, for height, width, and thickness. Wire mesh composed of 4.0 mm welded wires and spaced at 50 mm, were used to reinforce the slabs. Each push-out specimen has four 90 mm height TWP connectors embedded in the concrete slab. The TWP connector is composed of two CFS angles (L90×30×1.50 mm), connected with three M8 bolts, and reinforced by three φ8×300 mm transversal steel rebars. Each TWP shear connector is connected to the load distribution members with six M8 bolts. The dimensions and details of the TWC (Type C) push-out specimen are shown in Figure 4 and Figure 5. The referred-to specimen has the same components as the TWP specimens, except for the type of shear connector. In this context, the TWC shear connector consists of a 1.5 mm CFS lipped channel (C80×60×20) that is connected to the load distribution members with four M8 bolts.

The dimensions and details of the profiled steel sheet and lipped channel (Type D) push-out specimen are shown in Figure 6. The load distribution member in the referred-to specimen is composed of two lipped channels (C100×60×20×3.0 mm) connected with 3.0 mm CFS plates and M8 bolts. In this context, the shear connectors consist of 1.5 mm CFS lipped channels (C80×60×20). Each channel is connected to the web of the load distribution member with four M8 bolts. A profiled steel sheet with a thickness of 0.7 mm is placed between the shear connectors and the member. The concrete slabs have a thickness of 120 mm with the same dimensions and reinforcement as the TWP and TWC specimens. The experimental push-out tests were carried out after the concrete reached its full strength.

Figure 4: TWC (Type C) push-out specimen (dimensions in mm); a) section elevation, b) section side view, and c) section plan at A-A
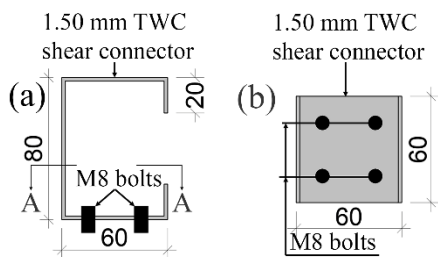
Figure 5: Details of the TWC (Type C) connectors; a) elevation, and b) section plan at A-A
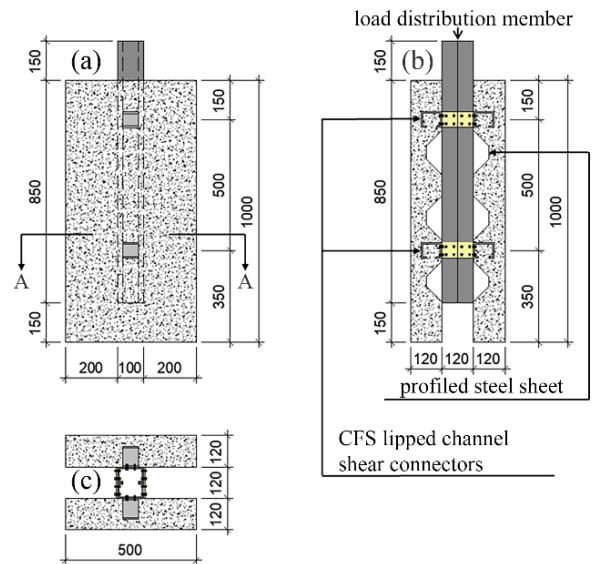
Figure 6: Steel sheet and lipped channels (Type D) push-out specimen (dimensions in mm); a) section elevation, b) section side view, and c) section plan at A-A

4.2 Setup of Push-Out Tests

Nine push-out specimens were tested using the available hydraulic actuator. The actuator had a load capacity of 2000 kN and was controlled by the MTS system. The loading protocol of the push-out tests was conducted according to the recommendations of Eurocode 4. Figure 7 shows the referred-to protocol, composed of two steps: (a) the initial cyclic loading step and (b) the final monotonic loading step.
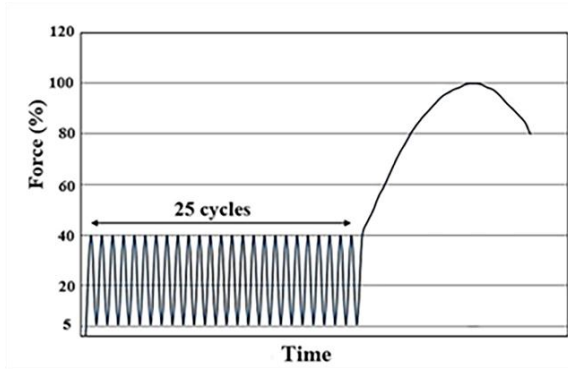
Figure 7: Loading protocol of the push-out tests

In the initial step, the hydraulic actuator was configured to operate in "force control" mode using the MTS system. The push-out specimens were subjected to a total of 25 cycles of loading and unloading, ranging from 5% up to 40% of the expected failure load. In the final step, the hydraulic actuator was configured to operate in "displacement control" mode, at a rate of 0.01 mm/s. The specimens were subjected to monotonic loading up to failure. To calculate the expected failure load accurately, three out of the nine push-out specimens (one for each type of shear connector) were only tested under a "displacement control" monotonic loading up to failure. The resulting load for each specimen was considered the expected failure load for the remaining two specimens. Figure 8 shows the experimental setup of the push-out test, including the load-transfer column and plate.
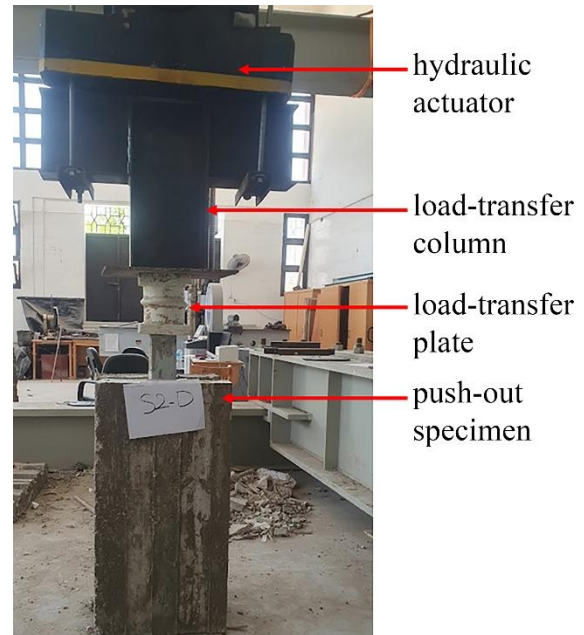
Figure 8: The setup of the push-out test

4.3 Results: Push-Out Tests

Table 2 lists the results of the tested specimens in terms of the failure load, ductility, maximum vertical displacement, and shear capacity for each connector. Based on the results, the failure mechanism of the TWP and TWC specimens was a separation between the load-transfer member and the concrete slab, as shown in Figure 9(a) and (b), respectively.

Table 2. Experimental results for the push-out specimens

Specimen	Loading Type	Failure Load (kN)		Max. Vertical Displacement d_{vsmax} (mm)	Ductility (mm)	Load Per One Shear Connector (kN)	
		Observed	Avg.			Observed	Avg.
S1-B	Monotonic	284.4				71.1	
S2-B	Cyclic - Monotonic	246.0	241.5	15.0	15.6	61.5	60.4
S3-B	Cyclic - Monotonic	237.0		16.1	16.7	59.3	
S1-C	Monotonic	229.5				57.4	
S2-C	Cyclic - Monotonic	203.6	209.4	10.6	17.8	50.9	52.4
S3-C	Cyclic - Monotonic	215.1		16.9	18.7	53.8	
S1-D	Monotonic	187.9				46.9	
S2-D	Cyclic - Monotonic	165.6	170.6	13.1	19.6	41.4	42.7
S3-D	Cyclic - Monotonic	175.5		17.2	19.8	43.9	

speration of the concrete slab

slippage between steel sheet and concrete slab
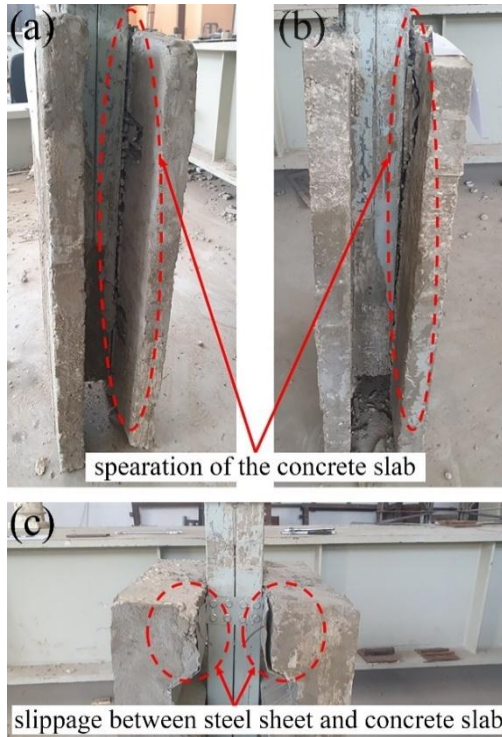
Figure 9: Failure mechanism in push-out specimens; a) TWP, b) TWC, and c) profiled steel sheet and lipped channel

The failure mechanism of the profiled steel sheet and lipped channel specimens was significant slippage between the concrete slab and the profiled steel sheet, as shown in Figure 9(c). The average failure load of the TWP specimens is 241.5 kN (60.4 kN for each TWP connector). The maximum vertical displacement value (d_{vsmax}) of the TWP specimens is 16.1 mm at the point

of failure. Furthermore, the minimum vertical displacement at 90% of the maximum load after failure, which is a measure of the ductility, is 15.6 mm. For TWC specimens, the average failure load is 209.4 kN, nearly 52.4 kN for each TWC connector, the maximum vertical displacement is 16.9 mm, and the ductility is 17.8 mm. For the profiled steel sheet and lipped channel specimens, the average failure load is 170.6 kN, about 42.7 kN for each connector, the maximum vertical displacement is 17.2 mm, and the ductility is 19.6 mm. According to the recommendations of Eurocode 4, shear connectors can be considered ductile if the displacement at 90% of the maximum load is equal to or greater than 6.0 mm. Therefore, all the proposed connectors can be considered safe in terms of deformation capacity. It must be noted that the Eurocode 4 recommendations are applied to class 1 and class 2 welded shear studs, where plastic design principles are used, however, most researchers used these recommendations for guidance. Based on the results, the TWP connectors showed the greatest shear capacity, while the profiled steel sheet and lipped channel connectors showed the lowest shear capacity. The observed shear capacity of the TWP is 15.3% higher than the TWC, while the TWC shear capacity is 22.7% higher than the profiled steel sheet and lipped channel connectors. Figure 10 shows the load vs. vertical displacement curves for S3-B, S3-C, and S3-D push-out specimens.
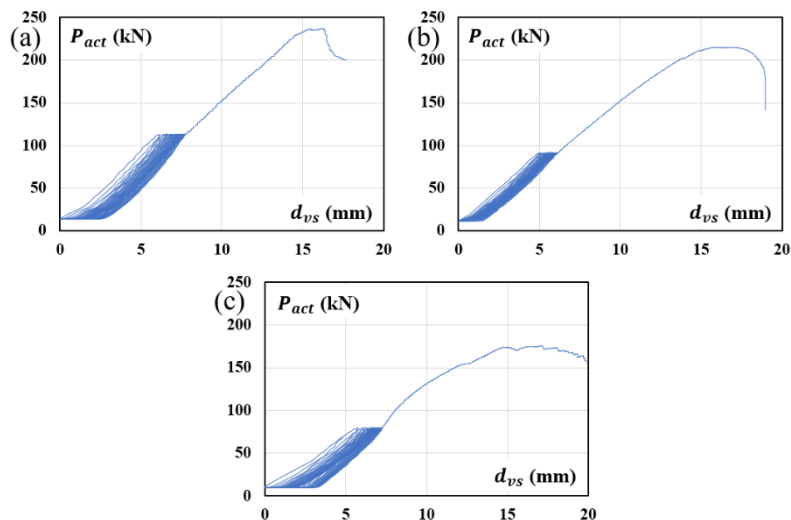
Figure 10: Load vs. vertical displacement curves for; a) S3-B, b) S3-C, and c) S3-D

7

Based on the previous results of the TWP specimens, the design equation derived by Oguejiofor et al. [27] showed a great agreement with the experimental results. The capacity of the proposed TWP connectors can be accurately determined based on the following equation:

$$Q_d = 4.5\, h_c\, t_c\, f_{ck} + 0.91\, A_{tr}\, f_y + 3.31\, n_h\, d^2\, \sqrt{f_{ck}} \quad (1)$$

Where Q_d is the design capacity of the connector, h_c is the height of the TWP, t_c is the thickness of the TWP, f_{ck} is the cylinder compressive strength of concrete, A_{tr} is the total area of the transversal rebars in the TWP, f_y is the yield stress of the transversal rebars, n_h is the number of holes in the TWP, and d is the diameter of the holes in the TWP. The designed capacity of the TWP connectors, according to the previous equation, is 60.1 kN, while the average shear capacity obtained from the present TWP push-out tests is 60.4 kN. For the TWC specimens, the design shear capacity can be calculated from the equation of hot-rolled channel connectors provided by AISC [28] as follows:

$$Q_d = 0.3\left(t_f + 0.5\, t_w\right) L_c \sqrt{f_{ck}\, E_{cm}} \quad (2)$$

Where t_f is the flange thickness of the channel, t_w is the web thickness of the channel, L_c is the length of the connector, and E_{cm} is the secant modulus of elasticity of concrete. The designed capacity based on that equation is 41.8 kN, while the average capacity based on the present TWC push-out tests is 52.4 kN. Therefore, the

design equation should be modified to accurately predict the shear capacity of the proposed TWC connectors. The modification of Equation 2 takes place by multiplying it by a factor which is the ratio between the experimental to designed load. This factor is equal to 1.25 and the modified equation should be as follows:

$$Q_d = 0.375\left(t_f + 0.5\, t_w\right) L_c \sqrt{f_{ck}\, E_{cm}} \quad (3)$$

In this case, the designed capacity is 52.2 kN which greatly agrees with the average experimental capacity. For lipped channel and steel sheet specimens, Equation 2 can be used to determine the shear capacity without modifications. The designed shear capacity, based on the previous equation, is 41.8 kN, while the average shear capacity from experimental push-out tests is 42.7 kN. Table 3 shows the relation between the designed and experimental shear capacity.

5 FULL-SCALE TESTS

5.1 Full-Scale Models: Fabrication and General Details

Sixteen full-scale models were fabricated and tested to study the behavior of CFS composite floor systems with the proposed shear connectors in terms of ultimate load-carrying capacity, maximum deformation, strain distribution at mid-section, and the factors affecting the failure mechanism of the CFS trusses. The naming convention for the full-scale models is shown in Figure 11.

Table 3. The relation between designed and experimental shear capacity

Specimen	Load Per One Shear Connector Q_u (kN)	Design Load Q_d (kN)	$\dfrac{Q_u}{Q_d}$
S2-B	61.5	60.1	1.02
S3-B	59.3	60.1	0.99
Average	60.4	60.1	1.01
S2-C	50.9	52.2	0.98
S3-C	53.8	52.2	1.03
Average	52.4	52.2	1.01
S2-D	41.4	41.8	0.99
S3-D	43.9	41.8	1.05
Average	42.7	41.8	1.02
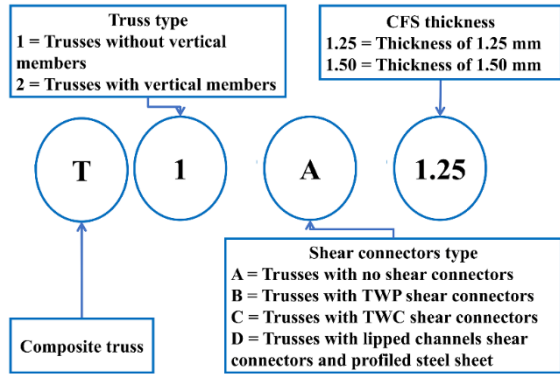
Figure 11: Naming convention for full-scale models

The CFS truss members were designed according to the recommendations of Eurocode 3 [29], [30], considering the reduction factors of safety. The design of CFS truss members considered the buckling effect of the top chord. However, the experimental results showed that using composite floor systems eliminates the top chord buckling problems, as the top chord was always subjected to tensile stresses during the experimental tests. Figure 12 shows the properties of the designed section for CFS truss members.

Figure 12: Properties of the designed section

The preparation of the full-scale models, shown in Figure 13(a), went through several stages: first, assembly of the CFS trusses, then preparation of the wooden formwork, next placement of the reinforcing steel mesh, and finally pouring, compacting, finishing, and curing of the concrete. Figure 13(b) shows the lateral view of the proposed full-scale models, with a total length of 5060

mm and a clear span of 5000 mm. The composite floor system consists of a CFS truss, a reinforced concrete slab on the top chord, and shear connectors to provide a significant interaction between the CFS truss and concrete slab. The CFS truss members were connected using CFS gusset plates and M8 bolts. The shear connectors are connected to the web of the top chord and located at the joints of the CFS truss. The CFS truss is composed of lipped channels (C100×60×20) with a thickness of 1.25 mm for eight full-scale models and 1.5 mm for the remaining eight models. To investigate the effect of the gusset plate thickness on the load-carrying capacity and failure mechanism of the CFS trusses, two gusset plate thicknesses, 1.25 mm, and 4.0 mm, were used to connect the truss members. However, all shear connectors have a uniform thickness of 1.5 mm. Figure 14 shows the cross-sectional views of the composite floor systems. The total width of the solid slab is 1000 mm, and the CFS truss, with a height of 460 mm, is aligned with the center of the slab. Two types of concrete slabs were used; the first one is of thickness 120 mm and poured into a profiled steel deck of thickness 0.7 mm with lipped channels shear connectors. While the other type is of 60 mm thickness poured into wooden formwork. The slab is reinforced with a 4.0 mm welded steel wire mesh spaced at 50 mm. The results of the push-out tests were used to estimate the required number of each type of connector to provide full interaction, according to the following equation by Eurocode 4:

$$\eta = \frac{n_c}{n_f} = \frac{R_q}{min\ of\ (R_c\ and\ R_t)} \tag{4}$$

Where:

$$R_q = n_c \times Q_u \tag{5}$$

$$R_c = 0.85 \times f_{ck} \times b_e \times t_s \tag{6}$$

$$R_t = A_g \times f_y \tag{7}$$

9
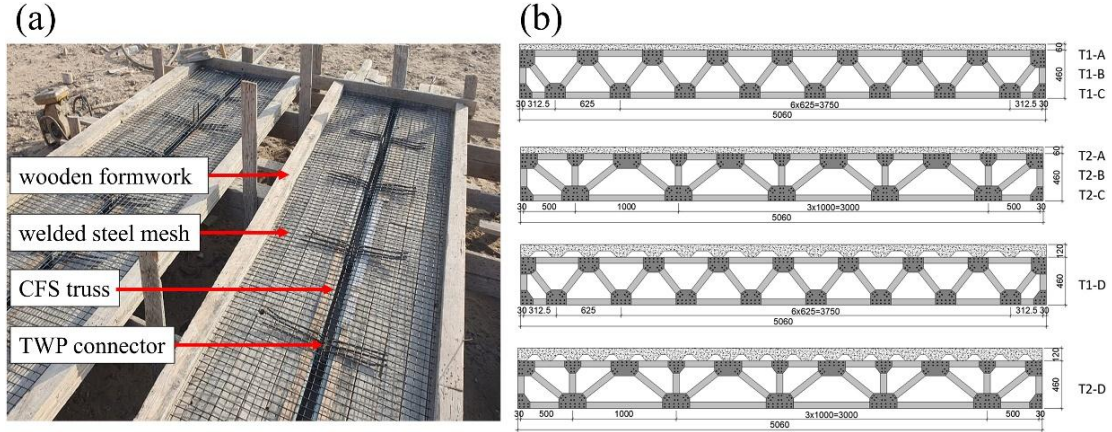
Figure 13: Full-scale models; a) general view before casting concrete, and b) lateral view (dimensions in mm)
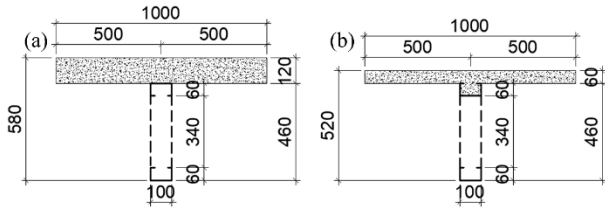
Figure 14: Cross-sectional view of the composite floor systems (dimensions in mm) for; a) T1-D and T2-D models, and b) remaining composite truss models

Where η is the degree of interaction, n_c is the number of shear connectors at the maximum shear zone, n_f is the number of shear connectors required for full interaction, R_q is the total capacity of shear connectors at the maximum shear zone, R_c is the maximum compressive force acting on the concrete, R_t is the maximum tensile force acting on the bottom chord, Q_u is the experimental capacity of the connector, b_e is the effective width of the slab, t_s is the thickness of the slab, and A_g is the gross area of the CFS section. f_y is the yield stress of the bottom chord. Table 4 shows the degree of interaction

for all full-scale models is greater than 1.0, which declares that the models should be able to provide full interaction between the concrete and CFS.

5.2 Setup of the Full-Scale Models

Sixteen full-scale models were subjected to two-point cyclic loading experimental tests to investigate the behavior of the composite CFS floor systems. The test setup, shown in Figure 15, consisted of a hot-rolled spreader beam and two transversal beams. The spreader beam was tightly connected to the actuator, so its weight was not added to the total experiment load. However, the weight of the transversal beams (0.5 kN per beam) was added to the total self-weight load (P_{sw}). The purpose of the transversal beams was to prevent the rotation of the tested models since the concrete slab was cast over a single CFS truss.

Table 4. Degree of interaction for each full-scale model

Specimen	n_c	Q_u (kN)	R_q (kN)	R_c (kN)	R_t (kN)	n_f (kN)	η
T1-B-1.25	3	60.4	181.2	1020.0	108.4	108.4	1.60
T2-B-1.25	4	60.4	241.6	1020.0	108.4	108.4	2.20
T1-B-1.50	3	60.4	181.2	1020.0	129.5	129.5	1.40
T2-B-1.50	4	60.4	241.6	1020.0	129.5	129.5	1.80
T1-C-1.25	3	52.4	157.2	1020.0	108.4	108.4	1.40
T2-C-1.25	4	52.4	209.6	1020.0	108.4	108.4	1.90
T1-C-1.50	3	52.4	157.2	1020.0	129.5	129.5	1.20
T2-C-1.50	4	52.4	209.6	1020.0	129.5	129.5	1.60
T1-D-1.25	3	42.7	128.1	1020.0	108.4	108.4	1.20
T2-D-1.25	4	42.7	170.8	1020.0	108.4	108.4	1.50
T1-D-1.50	3	42.7	128.1	1020.0	129.5	129.5	0.99
T2-D-1.50	4	42.7	170.8	1020.0	129.5	129.5	1.30

Figure 15: Test setup of the tested models; a) T1-C-1.5, and b) T2-D-1.25

The setup of the transversal beams across the clear span and the shape of the end supports are shown in Figure 16. The end supports used during the tests provided translation constraints only. It is important to highlight that one of the supports is left to permit horizontal translations in the longitudinal direction. To prevent premature bearing failure in CFS vertical truss members at supports, reinforcing members were introduced inside these members, located at the supports. The reinforcing members were composed of square hollow sections (SHS) with a thickness of 4.0 mm. The objective of the referred-to members, shown in Figure 17, was to transfer the reaction directly to the supports to prevent bearing failure of the CFS vertical truss members at the supports. Figure 18 shows the location of the vertical displacement transducer, which was used to measure the vertical deformation of the tested models during the test. The strain values were also measured during the test with Kyowa strain gauges that were installed on both the concrete slab and CFS truss members. Figure 18 also shows the setup of strain gauges on the CFS trusses. The strain gauges were installed as follows: one strain gauge on each of the first compression diagonal members (SG1 and SG2), two stain gauges on the bottom chord (SG3 and SG4), and two strain gauges on the top chord (SG5 and SG6). The strain gauges were installed on the webs of the referred-to members. Figure 19 shows the location of the strain gauges, which were installed on the concrete slab top surface near the mid-section (SG7 and SG8). The full-scale models were tested under a "displacement control" cyclic loading with the 2000 kN actuator.
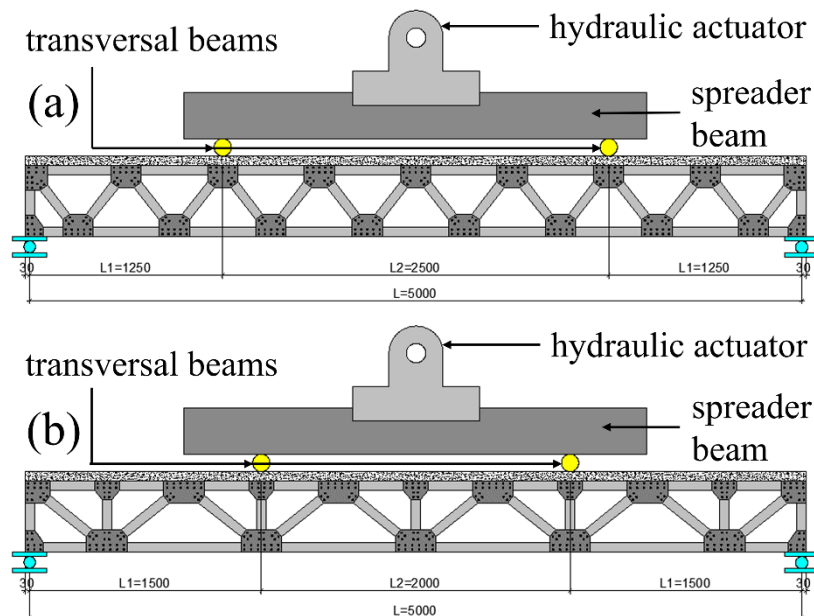
Figure 16: Experimental test Setup (dimensions in mm); a) T1 trusses, and b) T2 trusses
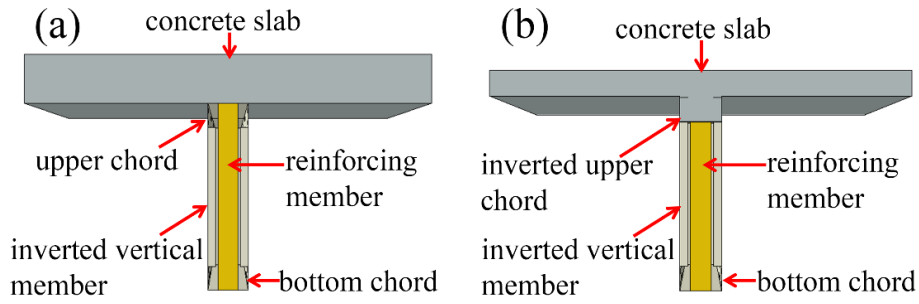
Figure 17: Details of the reinforcing member; a) T1-D and T2-D, and b) remaining truss models
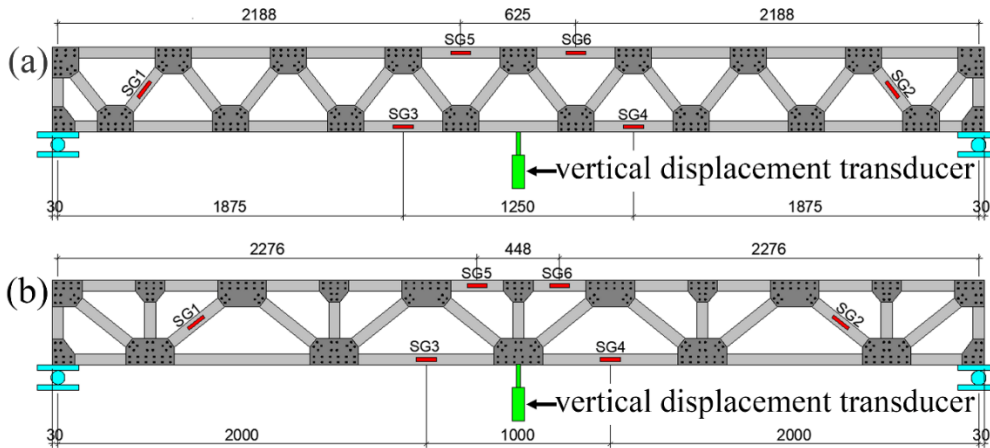
Figure 18: Location of the vertical transducer and strain gauges (dimensions in mm); a) T1 trusses, and b) T2 trusses
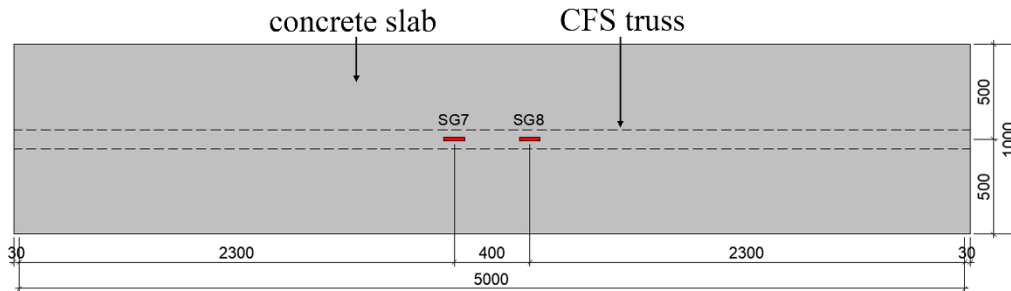
Figure 19: Location of strain gauges on the concrete slab

The loading protocol, as proposed by García et al. [31], is shown in Figure 20. The referred-to protocol is composed of increasing deflection amplitudes in constant increments of 1.0 mm, starting from 1.0 mm and continuing until the failure of the models. The deflection amplitudes used were 1.0 mm, 2.0 mm, 4.0 mm, 6.0 mm, 8.0 mm, and so on. For each value of displacement amplitude, a total of three compression cycles were applied. The loading rate remained constant during the test and was equal to 0.05 Hz.
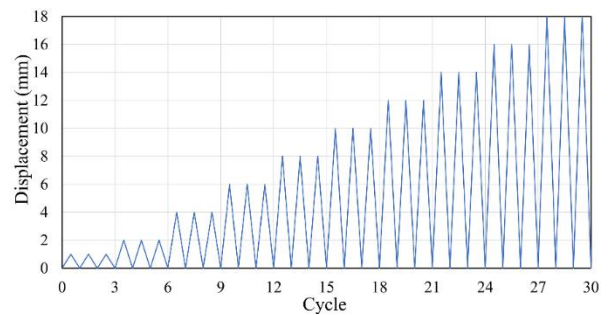
Figure 20: Cyclic loading protocol

5.3 Results: Full-Scale Tests

The full-scale test results showed important information about the behavior of the composite CFS trusses in terms of failure mechanisms, ultimate load-carrying capacity, and maximum deformation. The results of the full-scale models showed that three of the four proposed shear connectors provided almost full interaction between the concrete slab and the CFS truss, as no cracks were shown in the concrete slab, no separation happened between the slab and the CFS truss, and no buckling happened in the top chord. Table 5 lists the obtained experimental results of the sixteen full-scale models. P_{act} is the actuator load at failure, P_{sw} is the total self-weight of both the composite CFS truss model and transversal beams, P_u is the total experimental load, P_d is the calculated design load, and d_{vmax} is the maximum deformation observed at the point of failure, as measured by the vertical displacement transducer. The experimental test results in Table 5 show that the total load is always greater than the calculated design load, i.e., the ratio P_u/P_d is always greater than 1.

For models with type A shear connectors, there was a significant slippage and separation between the slab and the CFS truss at the maximum shear zone, as shown in Figure 16 at distance L_1. For the remaining models, there was almost a full interaction between the slab and the CFS from the beginning of the test up to failure, with no cracks observed on the concrete slab. The results showed that the thickness of the gusset plates was the main factor affecting the failure mechanism and ultimate load-carrying capacity of the composite CFS floor system. The thickness of the gusset plates in each model is shown in Table 5.

The gusset plates for T1-D-1.5 and T2-D-1.5 had a uniform thickness of 1.25 mm. The insignificant thickness of the referred-to gusset plates resulted in premature failure of the CFS truss connection, as shown in Figure 21(a), with a total load of 83.8 kN and 80.8 kN, respectively. However, for T1-D-1.25 and T2-D-1.25, the gusset plates had a uniform thickness of 4.0 mm. The load-carrying capacity of the composite floor systems was greatly enhanced by increasing the thickness of the gusset plates. The failure in this case occurred due to buckling of the diagonal members, as shown in Figure 21(b), with a total load of 100.8 kN and 94.1 kN, respectively.

Table 5. The experimental results of the full-scale models

Specimen	Gusset Plate Thickness (mm)		Actuator Load	Self-Weight Load	Total Load	Design Load	Ratio	Maximum Deformation
	Top Chord	Bottom Chord	P_{act} (kN)	P_{sw} (kN)	P_u (kN)	P_d (kN)	P_u/P_d	d_{vmax} (mm)
T1-A-1.25	1.25	4.0	78.4	10.0	88.4	68.0	1.3	32.0
T2-A-1.25	1.25	4.0	70.1	10.0	80.1	60.0	1.34	44.0
T1-A-1.50	1.25	4.0	95.8	10.3	106.1	96.0	1.11	45.9
T2-A-1.50	1.25	4.0	92.0	10.3	102.3	82.0	1.25	55.0
T1-B-1.25	1.25	4.0	84.9	10.0	94.9	68.0	1.4	60.9
T2-B-1.25	1.25	4.0	82.5	10.0	92.5	60.0	1.55	76.2
T1-B-1.50	1.25	4.0	102.1	10.3	112.4	96.0	1.18	67.5
T2-B-1.50	1.25	4.0	98.9	10.3	109.2	82.0	1.34	82.2
T1-C-1.25	1.25	4.0	79.1	10.0	89.1	68.0	1.32	68.1
T2-C-1.25	1.25	4.0	75.8	10.0	85.8	60.0	1.43	84.7
T1-C-1.50	1.25	4.0	98.1	10.3	108.4	96.0	1.13	77.0
T2-C-1.50	1.25	4.0	96.8	10.3	107.1	82.0	1.31	87.1
T1-D-1.25	4.0	4.0	87.5	13.3	100.8	70.0	1.44	42.3
T2-D-1.25	4.0	4.0	80.8	13.3	94.1	66.0	1.43	47.6
T1-D-1.50	1.25	1.25	70.5	13.3	83.8	80.0	1.05	50.1
T2-D-1.50	1.25	1.25	67.5	13.3	80.8	78.0	1.04	54.6
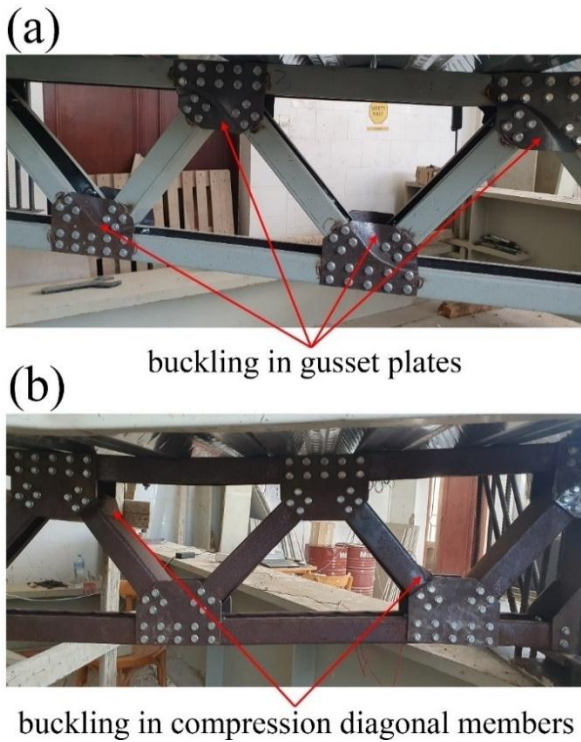
Figure 21: Failure mechanism for; a) T1-D-1.5, and b) T1-D-1.25

Increasing the thickness of gusset plates led to a greater load-carrying capacity, with an average increase of 18.4%, despite the value of the CFS member thickness. In the remaining models, the utilization of 1.25 mm gusset plates at the top chord and 4.0 mm plates at the bottom chord resulted in a failure mechanism characterized by buckling in both compression diagonal members and gusset plates of the top chord, as shown in Figure 22. The results also showed the effect of the member thickness on the load-carrying capacity of the CFS trusses. Trusses with a CFS members' thickness of 1.5 mm, as shown in Figure 23(a), showed greater load-carrying capacity compared to trusses with a members' thickness of 1.25 mm, as shown in Figure 23(b), with an average increase of 21.8% that is about the increase in the value of member cross-sectional area. It should be noted that, for all models, trusses without vertical members, T1-trusses, as shown in Figure 23(a), showed greater load-carrying capacity compared to trusses with vertical members, T2-trusses, as shown in Figure 23(b), with an average increase of 4.4%.
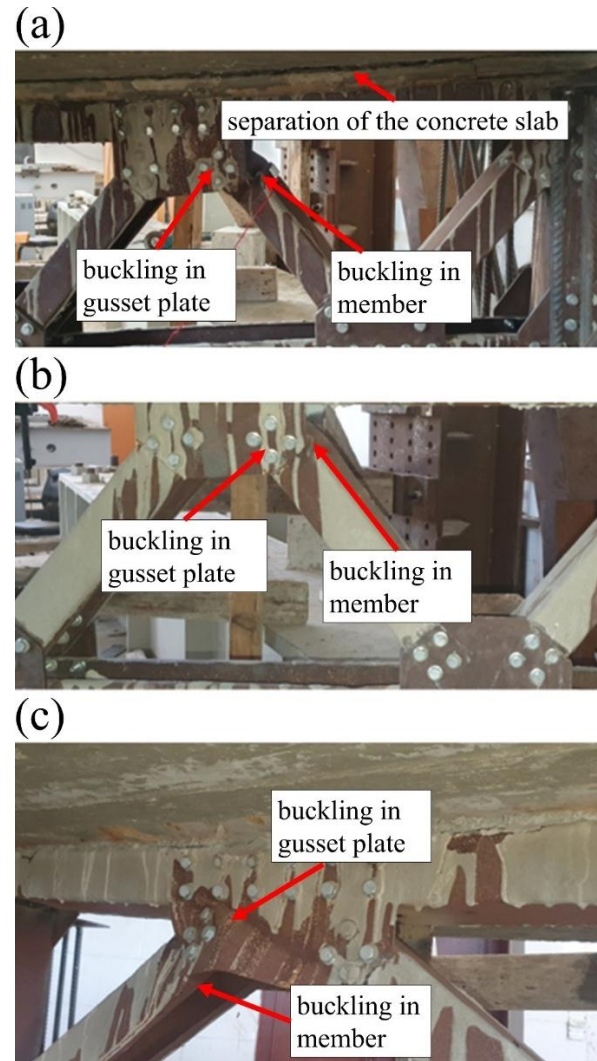
Figure 22: Failure mechanism of the full-scale models; a) T1-A-1.25, b) T1-B-1.5, and c) T2-C-1.25
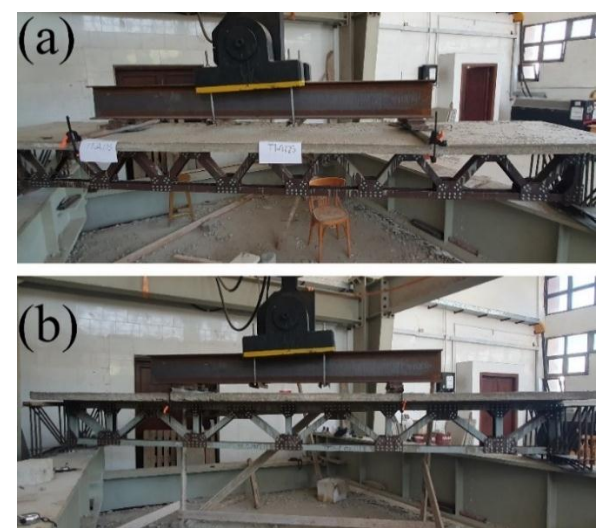
Figure 23: Full-scale test models; a) T1-A-1.25, and b) T2-C-1.5

14

It is important to acknowledge that models with TWP connectors showed greater load-carrying capacity compared to the remaining models, while models with TWC connectors showed higher vertical deformation. The maximum load measured was 112.4 kN for T1-B-1.5, and the maximum vertical deformation was 87.1 mm (L/57.5) for T2-C-1.5. The deformation of T2-C-1.5 is shown in Figure 24.

Figure 25 shows the actuator load (P_{act}) vs. vertical displacement (d_v) curves for some full-scale models at the mid-section. The results of the plots showed that, for all models, there was a linear behavior up to 17.5 kN. Above this load, there was a combination of the non-linear behavior of the concrete slab with the linear behavior of the CFS truss.

For model T1-A-1.25, the slab cracked, and separation between the slab and CFS began to develop at a load of 61.0 kN. As loading carried on, the system acted as a bare CFS truss. At a load of 63.5 kN, there was a slight buckling in some gusset plates of the top chord.
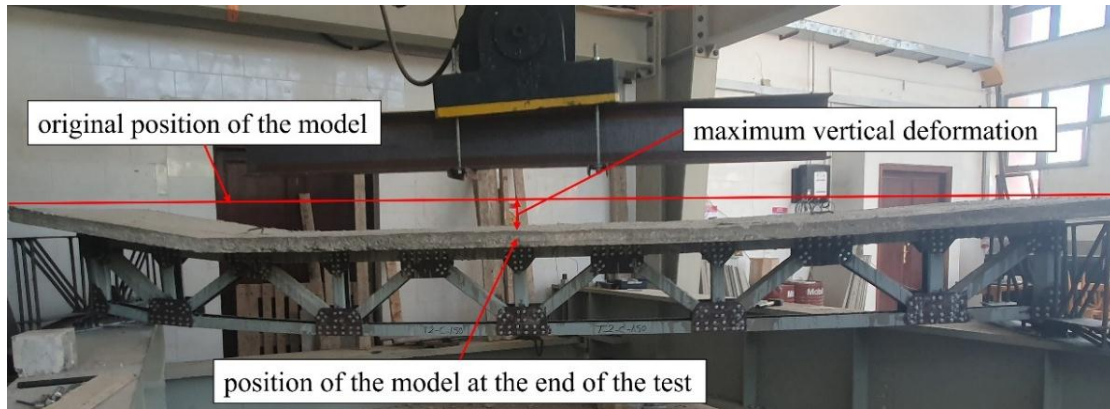
Figure 24: Maximum vertical deformation for T2-C-1.5 model
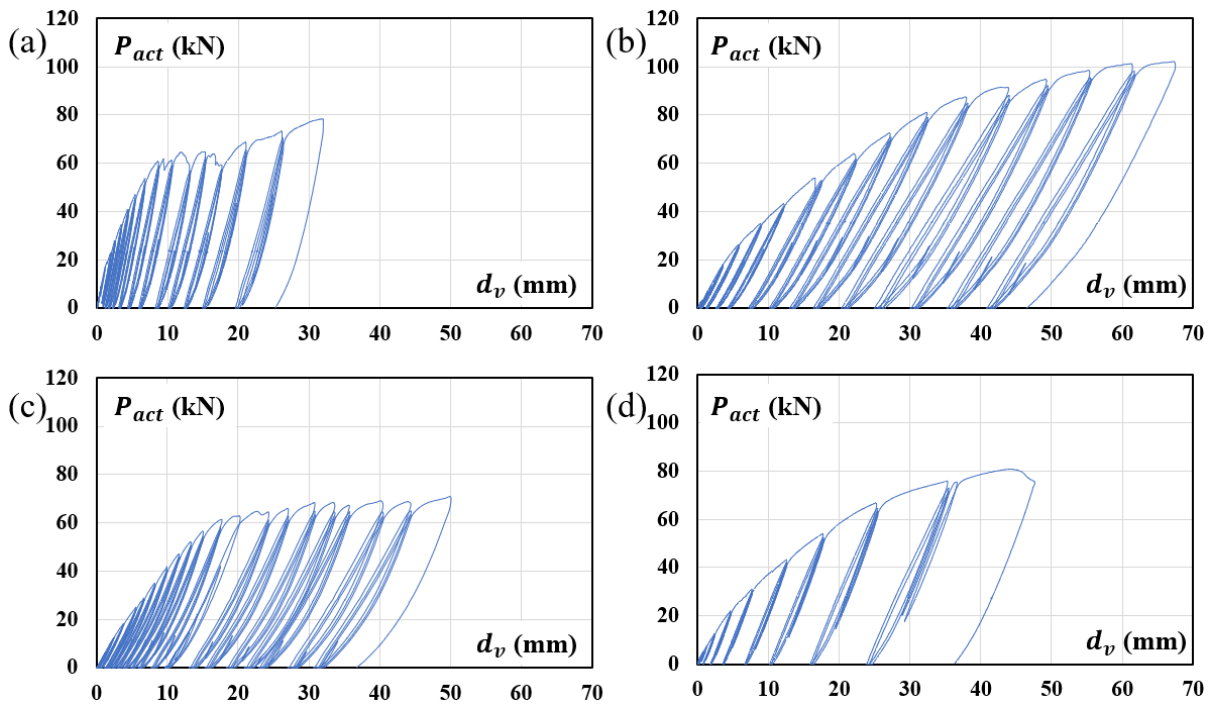
Figure 25: Load vs. vertical displacement curves for models; a) T1-A-1.25, b) T1-B-1.5, c) T1-D-1.5, and d) T2-D-1.25

The loading increase carried on until the CFS truss showed yielding deformation, represented in the buckling of the first compression diagonal members at a failure load of 78.4 kN. The failure mechanism of the referred-to model is shown in Figure 22(a). For model T1-B-1.5, at a load of 91.3 kN, there was a slight buckling in some gusset plates of the top chord. The loading step carried on until buckling of the first compression diagonal members occurred at a failure load of 102.1 kN. The failure mechanism of the referred-to model is shown in Figure 22(b) and (c). For model T1-D-1.5, at a load of 64.5 kN, buckling occurred in the gusset plates of both the top and bottom chords. The loading continued until premature failure occurred at a load of 70.5 kN due to the insignificant thickness of the gusset plates. The failure mechanism of the referred-to model is shown in Figure 21(a). For model T2-D-1.25, the loading continued, with no sign of buckling of the gusset plates until buckling of the first compression diagonal members began to develop at a load of 68.0 kN, and up to failure at a load of 80.8 kN. The failure mechanism of the referred-to model is shown in Figure 21(b). Figure 26 shows the average strain values, measured with Kyowa strain gauges, across the height of the models near the middle of the truss span section. The strain values showed that the depth of the neutral axis,

measured from the surface of the slab, for model T1-A-1.25 ranged from 100.0 mm at a load of 17.5 kN to 80.0 mm at a failure load of 78.4 kN, as shown in Figure 26(a). For model T1-B-1.5, the depth of the neutral axis ranged from 95.0 mm at a load of 17.5 kN to 55.0 mm at a failure load of 102.1 kN, as shown in Figure 26(b). For model T1-D-1.5, the depth of the neutral axis ranged from 80 mm at a load of 17.5 kN to 60.0 mm at a failure load of 70.5 kN, as shown in Figure 26(c). For model T2-D-1.25, the depth of the neutral axis ranged from 80.0 mm at a load of 17.5 kN to 55.0 mm at a failure load of 80.8 kN, as shown in Figure 26(d). Based on the previous results, it can be noted that the location of the neutral axis varies during the loading steps. It is important to highlight that the measured strain values did not include the initial strain caused by the total self-weight of both the model and transversal beams.

Finally, for all models excluding models with type A shear connectors, the location of the neutral axis was always in the concrete slab at all loading steps. The CFS chords were always subjected to axial tension without any observed buckling in the top chord. This enhanced the load-carrying capacity of the composite CFS system and proved that there was almost a full interaction between CFS and concrete in the proposed composite floor systems.
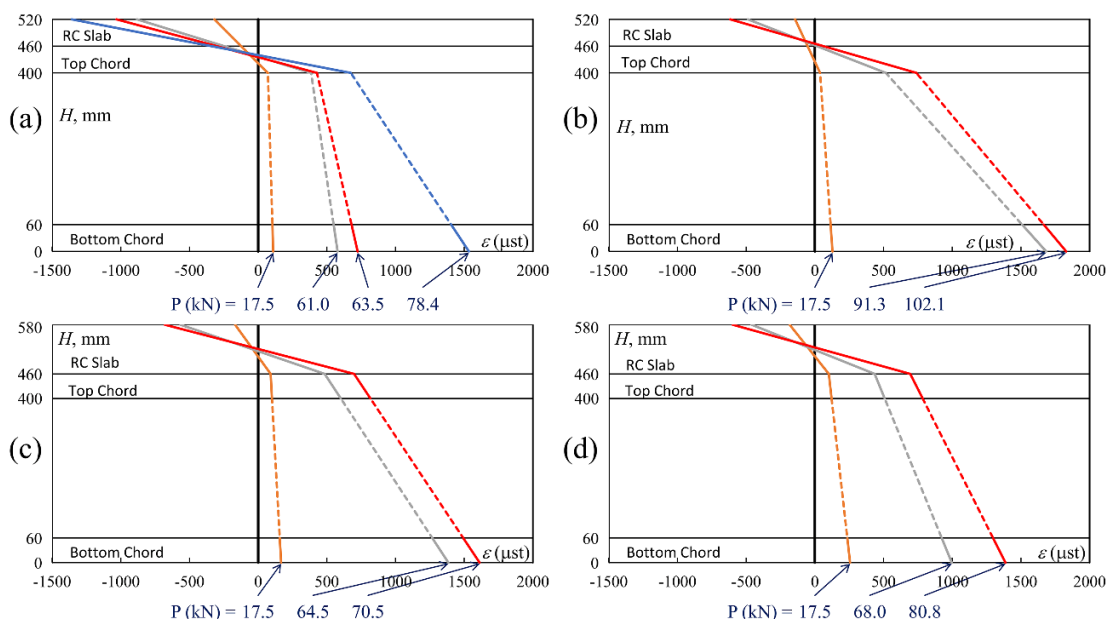
Figure 26: Strain vs. height at mid-section of the models; a) T1-A-1.25, b) T1-B-1.5, c) T1-D-1.5, and d) T2-D-1.25

6   CONCLUSIONS

This experimental research was carried out to investigate the behavior of the composite CFS truss and one-way concrete solid slab floor systems subjected to cyclic loading. Two groups of experimental tests were carried out. First, was the push-out test group to show the resistance of the CFS shear connectors to cyclic loading. The second was the full-scale composite CFS trusses and RC slabs with different truss arrangements, gusset plate thickness, member thickness, shear connector type, and concrete slab type. The major conclusions drawn from the current test results are as follows:

- The test results showed that three out of the four proposed solutions could be used in composite floor systems, as they guaranteed full interaction between the CFS and concrete, resulting in enhanced structural behavior of the composite systems. The referred solutions were: TWP, TWC, and CFS lipped channels placed over a profiled steel sheet.
- The push-out tests showed that the TWP shear connectors had the greatest shear capacity, while the shear connectors of CFS lipped channels placed over a profiled steel sheet had the lowest shear capacity.
- To estimate the shear capacity of different types of shear connectors, two previously proposed equations were verified. The equation proposed by Oguejiofor et al. gives a good estimation of the TWP connectors. While the AISC equation could be used for TWC connectors after calibration using a factor of 1.25. Finally, for slabs with steel decking, the AISC equation could be used without modifications.
- The full-scale test results showed that models with type A shear connectors did not provide significant interaction between the truss top chord and the concrete slab, as the concrete slab cracked and separated from the CFS truss. For the rest of the models, there was almost full interaction between the CFS and concrete, with no sign of cracks or separation observed in the concrete slab during the tests.

- The models with TWP shear connectors showed greater load-carrying capacity compared to the other models. However, models with TWC shear connectors showed higher vertical deformation compared to the remaining models.
- The thickness of the CFS truss members had a great effect on the load-carrying capacity of the composite CFS floor system. The load-carrying capacity was enhanced by an average of 21.8% when the thickness was increased from 1.25 mm to 1.5 mm. However, the shape of the truss had a slight effect on the load-carrying capacity. The utilization of T1-trusses enhanced the capacity by an average of 4.4%.
- The thickness of gusset plates was the main factor affecting the behavior of composite CFS floor systems in terms of failure mechanism and load-carrying capacity. The use of 4.0 mm gusset plates in both top and bottom chords prevented the premature failure of the CFS truss connections and enhanced the load-carrying capacity by an average of 18.4%.
- Finally, to achieve the optimal structural behavior of the composite CFS floor systems, it is recommended to use a CFS truss with a significant thickness (1.5 mm in this case) and without any vertical members (the T1-truss). Furthermore, it is recommended to use gusset plates with a significant thickness (4.0 mm in this case) to prevent premature failure at the connections, represented in the buckling of the gusset plates. In addition, the utilization of TWP shear connectors is recommended to provide full interaction between the CFS truss and the concrete solid slab.
- Full details of the experimental models and specimens are available in the thesis [32].

Conflicts of Interest

The authors state that there are no conflicts of interest regarding the publication of this research.

REFERENCES

[1] R. Sonnenschein, K. Gajdosova, and S. Gramblicka, "Comparison of composite, steel and reinforced concrete columns," *IOP Conf. Ser. Mater. Sci. Eng.*, vol. 960, no. 3, 2020, doi: 10.1088/1757-899X/960/3/032093.

[2] M. Surendar and M. S. Deepak, "Shear Connection between Steel and Concrete in Composite Structure," *Int. J. Innov. Technol. Explor. Eng.*, vol. 8, no. 12S, pp. 17–23, 2019, doi: 10.35940/ijitee.l1014.10812s19.

[3] P. C. Wang and D. J. Kaley, "Composite action of concrete slab and open-web joist (without the use of shear connectors). AISC Engineering Journal, Vol. 4, nO1.," 1967.

[4] M. H. Azmi and H. Robinson, "Composite Open-Web Trusses With - Metal Cellular Floor," *Can. J. Civ. Eng.*, vol. 5, no. March, p. 11, 1972.

[5] E. H. Fahmy, "Inelastic Analysis of Composite Open-web Steel Joists, M.S. Thesis, McMaster University, Hamilton, Ontario, Canada," 1974.

[6] T. Sharaf, M. Abdellatif, M. Elghandour, and A. ElSabbagh, "Experimental and finite element evaluations of single-T composite cold-formed steel beam with concrete slab," *Eng. Struct.*, vol. 318, no. May, p. 118762, 2024, doi: 10.1016/j.engstruct.2024.118762.

[7] A. M. I. Muhammad, "Scholarship at UWindsor Behaviour of Open Web Steel Joist in Composite Deck Floor System Behaviour of Open Web Steel Joist in Composite Deck Floor System," 2015.

[8] G. Merryfield, A. El-Ragaby, and F. Ghrib, "New shear connector for Open Web Steel Joist with metal deck and concrete slab floor system," *Constr. Build. Mater.*, vol. 125, pp. 1–11, 2016, doi: 10.1016/j.conbuildmat.2016.08.006.

[9] M. S. Abduljabbar, M. J. Hamood, and W. S. Abdulsahib, "Flexural behavior of composite open web steel joist and concrete slab," *IOP Conf. Ser. Mater. Sci. Eng.*, vol. 737, no. 1, 2020, doi: 10.1088/1757-899X/737/1/012017.

[10] L. A. A. de S. Leal and E. de M. Batista, "Civil Engineering Composite floor system with CFS trussed," *REM - Int. Eng. J.*, vol. 73, no. 1, pp. 23–31, 2020.

[11] J. R. U. Mujagic, W. S. Easterling, and T. M. Murray, "Design and behavior of light composite steelconcrete trusses with drilled standoff screw shear connections," *J. Constr. Steel Res.*, vol. 66, no. 12, pp. 1483–1491, 2010, doi: 10.1016/j.jcsr.2010.06.001.

[12] M. Dabaon and M. F. Hassanein, "Behavior of Shear Connectors Using Normal and High Strength Concrete" Part(1) Experimental study," in *11th ICSGE (Eleventh international colloquium on structural and geotechnical Engineering,Ain Shams University, Cairo, Egypt.*, Dabaon, M., 2005.

[13] E. E. Etman, M. A. Dabaon, and A. M. Taha, "Behaviour of High Strength Concrete Composite Slabs With Different End Anchorages," *J. Eng. Res.*, vol. 1, no. 2015, pp. 121–141, 2015, doi: 10.21608/erjeng.2015.126811.

[14] M. Dabaon, M. H. El-Boghdadi, O. F. Kharoob, and A. H. El Gendy, "Experimental Shear Resistance Evaluation of Ordinary and Perfobond Y-Shaped Shear Connectors," *J. Eng. Res.*, vol. 1, no. 2015, pp. 142–154, 2015, doi: 10.21608/erjeng.2015.126812.

[15] S. E. Abd-Rabon and M. Daboan, "Comparison between Theoretical and Experimental Investigation of Composite Beams with Spiral Shear Connectors.(Dept.C)," *MEJ. Mansoura Eng. J.*, vol. 20, no. 1, pp. 22–37, 2021, doi: 10.21608/bfemu.2021.159966.

[16] N. Wehbe, P. Bahmani, and A. Wehbe, "Behavior of Concrete/Cold Formed Steel Composite Beams: Experimental Development of a Novel Structural System," *Int. J. Concr. Struct. Mater.*, vol. 7, no. 1, pp. 51–59, 2013, doi: 10.1007/s40069-013-0031-6.

[17] C. T. T. Hsu, S. Punurai, W. Punurai, and Y. Majdi, "New composite beams having cold-formed steel joists and concrete slab," *Eng. Struct.*, vol. 71, pp. 187–200, 2014, doi: 10.1016/j.engstruct.2014.04.011.

[18] S. O. Bamaga, M. M. Tahir, C. S. Tan, P. N. Shek, and R. Aghlara, "Push-out tests on three innovative shear connectors for composite cold-formed steel concrete beams," *Constr. Build. Mater.*, vol. 223, pp. 288–298,

2019, doi: 10.1016/j.conbuildmat.2019.06.223.

[19] L. A. A. de S. Leal and E. de M. Batista, "Experimental investigation of composite floor system with thin-walled steel trussed beams and partially prefabricated concrete slab," *J. Constr. Steel Res.*, vol. 172, 2020, doi: 10.1016/j.jcsr.2020.106172.

[20] M. Hosseinpour, M. Zeynalian, A. Ataei, and M. Daei, "Push-out tests on bolted shear connectors in composite cold-formed steel beams," *Thin-Walled Struct.*, vol. 164, no. September 2020, p. 107831, 2021, doi: 10.1016/j.tws.2021.107831.

[21] J. L. Dawe, Y. Liu, and J. Y. Li, "Strength and behaviour of cold-formed steel offset trusses," *J. Constr. Steel Res.*, vol. 66, no. 4, pp. 556–565, 2010, doi: 10.1016/j.jcsr.2009.10.015.

[22] M. C. H. Yam and J. J. R. Cheng, "Behavior and design of gusset plate connections in compression," *J. Constr. Steel Res.*, vol. 58, no. 5–8, pp. 1143–1159, 2002, doi: 10.1016/S0143-974X(01)00103-1.

[23] M. Reda, T. Sharaf, A. ElSabbagh, and M. ElGhandour, "Behavior and design for component and system of cold-formed steel roof trusses," *Thin-Walled Struct.*, vol. 135, no. April 2018, pp. 21–32, 2019, doi: 10.1016/j.tws.2018.10.038.

[24] R. Padmanaban and S. Suresh, "Experimental Study on use of Cold Formed Steel Sections as Truss Members," *Int. J. Innov. Technol. Explor. Eng.*, no. 6, pp. 101–106, 2019.

[25] M. I. Z. Ammar, D. Irawan, D. Iranata, and B. Suswanto, "Study analysis on failure mechanism of small span pedestrian cold formed truss bridge," *Int. J. Eng. Res. Technol.*, vol. 13, no. 7, pp. 1757–1763, 2020, doi: 10.37624/ijert/13.7.2020.1757-1763.

[26] CEN, "Eurocode 4: Design of Composite Steel and Concrete Structures – Part 1-1: General Rules and Rules for Buildings," Brussels, Belgium, EN 1994-1-1, 2004.

[27] E. C. Oguejiofor and M. U. Hosain, "Numerical analysis of push-out specimens with perfobond rib connectors," *Comput. Struct.*, vol. 62, no. 4, pp. 617–624, 1997, doi: 10.1016/S0045-7949(96)00270-2.

[28] AISC, "Specification for Structural Steel Buildings," Chicago, IL, USA, ANSI/AISC 360-16, 2016.

[29] CEN, "Eurocode 3: Design of Steel Structures – Part 1-3: General Rules – Supplementary Rules for Cold-Formed Members and Sheeting," Brussels, Belgium, EN 1993-1-3, 2006.

[30] CEN, "Eurocode 3: Design of Steel Structures – Part 1-5: Plated Structural Elements," Brussels, Belgium, EN 1993-1-5, 2006.

[31] J. M. García, R. L. Bonett, A. E. Schultz, J. Carrillo, and C. Ledezma, "Flexural behavior of ungrouted post-tensioned concrete masonry beams with unbonded bars," *Constr. Build. Mater.*, vol. 203, no. January, pp. 210–221, 2019, doi: 10.1016/j.conbuildmat.2018.12.101.

[32] M. Elaraby, A. ElSabbagh, T. Sharaf, and M. ElGhandour, "Experimental Study of Composite Cold-Formed Steel Trusses in Floor Systems Subjected to Cyclic Loading," MSc. Thesis, Port Said University, Port Said, Egypt, 2024.